Deploying Dynamic On-Board Signal Processing Schemes for Multibeam Satellite Systems

Vahid Joroughi*, Mirza Golam Kibria*, Eva Lagunas*, Bhavani Shankar M.R.*, Symeon Chatzinotas*, Joel Grotz†
Sina Maleki* and Björn Ottersten*
* The University of Luxembourg, Luxembourg †SES S.A., Betzdolf, Luxembourg
Email: {vahid.joroughi, mirza.kibria, eva.lagunas, bhavani.shankar, symeon.chatzinotas, sina.maleki, bjorn.ottersten}@uni.lu
joel.grotz@ses.com

***Abstract*—This paper designs dynamic on-board signal processing schemes in a multiple gateway multibeam satellite system where full frequency reuse pattern is considered among the beams and feeds. In particular, we deploy on-board Joint Precoding, Feed selection and Signal switching mechanism (JPFS) so that the following advantages are realized, I) No need of Channel State Information (CSI) exchange among the gateways and satellite, since the performance of precoding is highly sensitive to the quality of CSI, II) In case one gateway fails, rerouting signals through other gateways can be applied without any extra signal processing, III) Properly selecting on-board feed/s to serve each user which generates maximum gain toward corresponding user, IV) Flexibly switching the signals received from the gateways to requested users where each user can dynamically request traffic from any gateway, and V) Multiple user with multiple traffic streams can be dynamically served at each beam. However, deploying such JPFS architecture imposes high complexity to the satellite payload. To tackle this issue, this study aims at deploying JPFS that can provide affordable complexity at the payload. In addition, while increasing the data demand imposes extensive bandwidth resources requirement in the feeder link, the proposed JPFS design works efficiently with available feeder link resources even if the data demand increases. The proposed design is evaluated with a close-to-real beam pattern and the latest broadband communication standard for satellite communications.**

I. Introduction

The use of multiple spot beams (multibeam) satellites have been recently considered by applying fractional frequency reuse among beams. Such systems rely on employing a large number of beams instead of a single beam aiming at providing higher spectral efficiency [1, 2]. However, one of the major challenges in multibeam architecture lies in dealing with interference among adjacent beams due to the side lobes of the radiation pattern of beams on the Earth surface. To tackle this problem and even further increase the satellite system capacity, one promising solution is to use full frequency reuse pattern among beams by resorting to interference mitigation techniques such as precoding in the forward link and multi-user detection in the return link [3, 4]. However, the design of interference mitigation techniques is sensitive to the accuracy of Channel State Information (CSI). In addition, the interference mitigation technique is realized at transmitting segment (i.e. either in satellite or gateway) in order to keep user terminal complexity affordable.

Apart from interference on user side, meeting the user requirements imposes large spectral demands on the feeder link, i.e. the bidirectional link between the satellite and the gateway. In particular, assuming N antennas generating K beams each requiring a bandwidth of B_{beam} with $N \geq K$, it is shown that the feeder link bandwidth needs to be $\mathrm{B}_{\text{feeder-link}} = N\mathrm{B}_{\text{beam}}$. However, akin to user link, i.e. the bidirectional link between satellite and user terminals, the spectrum allocated to the feeder link is also limited, thereby rendering feeder link as a communication bottleneck. Note that in contrast to the single feed per beam architectures, i.e. $N = K$, applying Multiple Feeds per Beam (MFB) at the payload, i.e. $N \geq K$, can reduce the scan losses for a large continental coverage, and are specially suited for contour beams [5].

Recently, Multiple Gateway Processing (MGP) multibeam architecture has been considered as one of the key enablers to reduce the feeder link bandwidth requirements. This architecture exploits the multiplexing diversity by reusing all the available feeder link bandwidth across different gateways [5, 6]. As such, the required feeder link bandwidth becomes

$$\mathrm{B}_{\text{feeder-MGP}} = \frac{N}{F}\mathrm{B}_{\text{beam}}, \tag{1}$$

where F is the number of gateways, and $\mathrm{B}_{\text{feeder-MGP}}$ denotes the feeder link resources which is required at MGP. Clearly $\mathrm{B}_{\text{feeder-MGP}} < \mathrm{B}_{\text{feeder-link}}$ and the difference grows with F. Nevertheless, the current MGP architectures suffer from the following issues: **a)** deployment of MGP networks increases the cost of the system. Considering (1), by increasing the demand a specific number of gateways should be employed to satisfy the the increased demands with the associated feeder link bandwidth, **b)** Inter-feeder link interference in addition to the interference in the user link [5], **c)** The interference mitigation techniques should be deployed distributively among the gatways which typically leads to performance degradation [6]. Additionally, implementing the distributed interference mitigation techniques entails a CSI exchange mechanism among gateways, and **d)** Even if employing MGP architecture increase the outage probability where in case of gateway failure the traffic can be rerouted through other gateways, a costly and complex inter gateway communication is required to exchange data among gateways.

Contributions: This paper investigates the performance of the forward link of an MGP scheme where the following signal processing units are applied to the payload.

(a) On-Board Precoding: This unit is applied to mitigate interference in user link. Considering that the CSI of user link is time-varying, this paper focuses on the developing a fixed on-board precoding which is robust to the variations in user link CSI, aiming at preserving the payload complexity affordable. The variability of the user link channel components is assumed

due to the change of position of the users in consecutive time instants as well as time-varying atmospheric fading.

Remark 1. Even with highly directive antennas, the feeder links originating at different gateways are partially interfering. In this work we assume that gateways are sufficiently separated on the earth surface and space so that the inter-feeder link interference can be ignored.

(b) On-Board Signal Switching: This operation is applied to fulfill: **i)** Reducing the feeder link requirements in (1) to $\mathrm{B}_{\text{feeder-onboard}} = \frac{K}{F}\mathrm{B}_{\text{beam}}$, with $\mathrm{B}_{\text{feeder-onboard}} < \mathrm{B}_{\text{feeder-MGP}}$ whenever $N > K$. **ii)** Providing flexibility in order to switch signals received from the gateways to requested users. In this context, each user can dynamically request traffic from any gateway. **iii)** Multiple users with multiple traffic streams can be dynamically served at each beam. **iv)** A single signal can broadcast to multiple users that are geographically located at different beams.

(c) On-Board Feed Selection: This unit is employed in order to properly select on-board feed/s to serve each user which generates maximum gain toward corresponding user.

The MGP architecture containing (a)-(c) possibilities refers to on-board Joint Precoding, Feed Selection and Packet Switching (JPFS). Note that, in addition to (a)-(c), employing JPFS in MGP networks lead to a number additional advantages. First, no CSI feedback mechanism between satellite and gateways is necessary, leading to less CSI round trip. Second, to design interference mitigation techniques, no CSI exchange mechanism is required among the gateways. Third, in case one gateway fails, the traffic can be rerouted to the user terminals through other gateways without applying any extra signal processing schemes at the gateways.

Notation: Throughout this paper, the following notations are adopted. Boldface uppercase letters denote matrices and boldface lowercase letters refer to column vectors. $(.)^H$, $(.)^T$ and $(.)^+$ denote Hermitian, transpose, and diagonal (with positive diagonal elements) matrices, respectively. $\mathbf{I}_N$ builds the $N \times N$ identity matrix. $(\mathbf{A})_{ij}$ represents the (i-th, j-th) element of matrix $\mathbf{A}$. The notation $diag$ represents a diagonal matrix. If $\mathbf{B}$ is a $N \times N$ matrix, $\mathbf{A} \leq \mathbf{B}$ implies $\mathbf{A} - \mathbf{B} \leq 0$ is negative semidefinite. Finally, $\mathrm{E}\{.\}$ and $||.||$ refer to the expected value operator and the Frobenius norm operator, respectively.

II. Signal model

Herein, the focus is on the forward link of a MGP based multibeam satellite system, where a single Geosynchronous (GEO) satellite with multibeam coverage provides fixed broadband services to a large set of users with N feeds and K beams, configured corresponds to the MFB mode with $N > K$.

By employing a Time Division Multiplexing (TDM) scheme, at each time instant, a total of M single antenna users are simultaneously served within K beams by a set of F gateways. In such an architecture, it is conceived that

Unicast signal transmission: a set of L_1 users, with $L_1 = K$ and $L_1 < M$, which are uniformly distributed within K beams and receives individual traffic stream per user.

Broadcast signal transmission: a set of L_2 users receives a copy of signals which transmits to L_1 depending on each user requirement, with $M = L_1 + L_2$. Note that each user serves through a single feed, with $N = M = L_1 + L_2$ and $K < L_1 + L_2$.

Let us assume that the gateways use a full frequency reuse pattern at the user link among beams and feeds. Therefore, the interference among users is the bottleneck of whole system and applying precoding is essential. By assuming noiseless and perfectly calibrated feeder link among gateways (Remark 1), the overall received signals can be modeled as

$$\mathbf{y} = \mathbf{H}\mathbf{x} + \mathbf{n} \tag{2}$$

where $\mathbf{y} = \left(y_1, ..., , y_M\right)^T \in \mathbb{C}^{M\times 1}$ is a vector containing the received signals at M users within K beams. Vector $\mathbf{n} = \left(n_1, ..., n_M\right)^T \in \mathbb{C}^{M\times 1}$ contains the impact of noise at M user terminals. It is considered that the noise terms are Gaussian distributed with zero mean and unit variance so that $E\left\{\mathbf{n}\mathbf{n}^H\right\} = \mathbf{I}_M$. The vector $\mathbf{x} \in \mathbb{C}^{N\times 1}$ is a vector containing the transmitted signals to K beams. The matrix $\mathbf{H} \in \mathbb{C}^{M\times N}$ denotes the user link channel matrix. For notation convenience, it is better to define the channel vector of the i-th user as $\mathbf{h}_i \in \mathbb{C}^{1\times N}$ so that

$$\mathbf{H} = \left[\mathbf{h}_1^H, ..., \mathbf{h}_i^H, \ldots, \mathbf{h}_M^H\right]. \tag{3}$$

To show the weight of on-board JPFS, the transmitted symbol vector $\mathbf{x}$ in (2) can be decomposed as

$$\mathbf{x} = \mathbf{W}\mathbf{s}, \tag{4}$$

where $\mathbf{s} \triangleq \begin{pmatrix}\mathbf{s}_a \\ \mathbf{s}_b\end{pmatrix} \in \mathbb{C}^{M\times 1}$ is a vector that contains the transmitted symbols to M users so that $\mathbf{s}_a \in \mathbb{C}^{L_1\times 1}$ denotes the transmitted signals L_1 users in unicast mode and $\mathbf{s}_b \in \mathbb{C}^{L_2\times 1}$ is the transmitted signals to L_2 users in broadcast mode. In this context, we consider that the F gateways transmit K signals to the payload, $K = L_1$ where $\mathbf{s}_a = [\mathbf{s}_{a,1}, ..., \mathbf{s}_{a,f}, ..., \mathbf{s}_{a,F}]^T$ with $\mathbf{s}_{a,f} \in \mathbb{C}^{m_f\times 1}$ is the vector of transmitted symbols from f-th gateway, with $m_f < K$ and $K = \sum_{f=1}^{F} m_f$. In the sequel, the matrix $\mathbf{W} \in \mathbb{C}^{N\times K}$ indicates the weight of on-board JPFS. Indeed, the size of $\mathbf{W}$ is constructed to convert K feeder link signals to N on-board feed signals, leading to optimizing feeder link bandwidth resources and guaranteeing $\mathrm{B}_{\text{feeder-onboard}} = \frac{K}{F}\mathrm{B}_{\text{beam}}$. Then, we propose the following decomposition of $\mathbf{W}$:

$$\mathbf{W} = \sqrt{\alpha}\mathbf{W}_a\mathbf{W}_b\mathbf{W}_c, \tag{5}$$

where $\mathbf{W}_b$ of size $N \times K$ is on-board precoding scheme. The matrix $\mathbf{W}_a$ of size $N \times N$ and $\mathbf{W}_b$ of size $K \times K$ show the weight of on-board signal switching scheme and feed selection mechanism at the payload.

Proposition 1. To design $\mathbf{W}$ at the payload, rebuilding and detecting vector $\mathbf{s}_a$ collected from F gateways at the payload is essential. As a matter of fact, it entails establishing a precise synchronization and detection procedure between satellite and gateways aiming to detect arrival symbols, i.e. $\mathbf{s}_{a,f}$ from f-th gateway, $f = 1, ..., F$, and project them in vector $\mathbf{s}_a$. It is assumed that a perfect synchronization and detection procedure can be established between satellite and gateways with

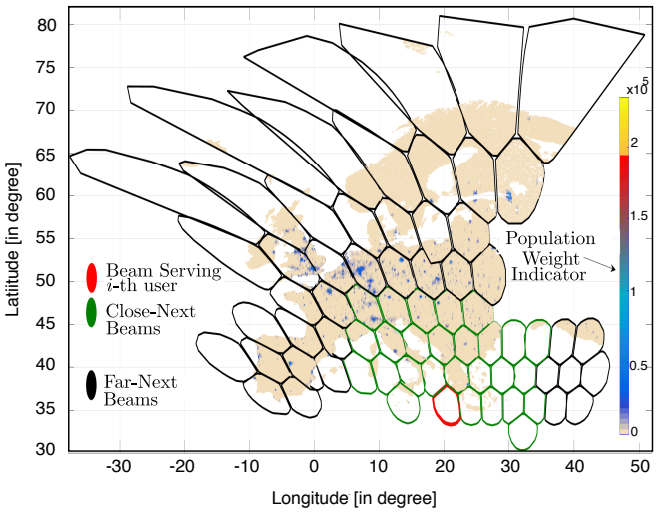

Fig. 1. Contour of the $K = 71$ beams covering whole Europe. The beam footprints have been generated in the framework of European Space Agency (ESA) SatNex IV project [8]. The footprint of the beam which serves i-th user, $i = 1, ...M$, 30 Close-Next beams and 40 Far-Next beams. The number of Close- and Far-Next beams can be obtained through numerical analyzing.

neglectable complexity. ■

For the sake of clarity and justify the necessity of applying $\mathbf{W}_c$ and $\mathbf{W}_a$, Figure 1 shows the population weight of each beam. It is seen that some beams have higher population weight than other. Therefore, beams with higher population requires higher service than the rest, leading to employ signal switching and feed selection as parts of JPFS matrix $\mathbf{W}$. The objective problem can be then formulated as

$$\begin{aligned} &\underset{\mathbf{W}}{\text{maximize}} \quad \sum_{i=1}^{M} r_i \\ &s.t. \quad \text{trace}\left(\mathbf{W}\mathbf{W}^H\right) \leq P, \end{aligned} \tag{6}$$

where r_i denotes the achievable rate of the i-th user, $r_i = \log_2(1 + \text{SINR}_i)$ and P denotes the total available power at the satellite. Denoting $\mathbf{w}_i$ corresponds to the i-th column of matrix $\mathbf{W}$, the notation SINR_i is the Signal to Interference pulse Noise Ratio (SINR) at i-th user and can be expressed as

$$\text{SINR}_i = \frac{|\mathbf{h}_i^H \mathbf{w}_i|^2}{\sum_{j \neq i}^{M} |\mathbf{h}_i^H \mathbf{w}_j|^2 + 1}. \tag{7}$$

III. Designing On-Board JPFS Matrix $\mathbf{W}$

This section aims at providing designing of $\mathbf{W}$. Here, we put stress of a design of $\mathbf{W}$ which can support a good trade off between complexity and performance.

As a matter of fact, complexity of designing $\mathbf{W}$ comes from: (i) *component complexity,* computational complexity of calculating the components included in $\mathbf{W}$ itself, (ii) *CSI acquisition complexity,* acquiring real time CSI at the satellite while channel matrix is time varying. Therefore, the proposed design of $\mathbf{W}$ shall overcome difficulties in (i) and (ii) while it provides acceptable performance. In the following, we aim at proposing possible solution to reduce the complexities in (i) and (ii).

A. Reducing component complexity

For a moment let us consider that $\mathbf{W}$ performs only as on-board precoding scheme in order to mitigate interference among users in the user link and other flexibilities (on-board signal switching and feed selection) are not neglected, i.e. $\mathbf{W}_a = \mathbf{I}_N$, $\mathbf{W}_c = \mathbf{I}_K$ and

$$\mathbf{W} = \sqrt{\alpha}\mathbf{W}_b. \tag{8}$$

Now, for sake of achieving a good trade off between keeping low complexity of deployed $\mathbf{W}$ at the payload and properly mitigating interference received by i-th user ($i = 1, .., M$) it is conceived that: i-th user receives interference from users located at Close-Next beams and no (or at least negectable) interference from users at Far-Next beams. Close- and Far-Next beams respectively refer to the beams which generate strong interference and weak interference on the beam that i-th user located on. Indeed, the Close-Next beams create high levels of interference due to their closet footprint and side lobes of radiation pattern to beam which serves i-th user on the Earth surface while Far-Next beams have far radiation pattern and footprint.

For the sake of clarity, Figure 1 depicts the footprints of Close- and Far-Next beams which are surrounded the beam which serves i-th user. In this context, denoting D_C and D_F (with $N > D_F, N > D_C$) as the total number of feeds which respectively serve users within Close- and Far-Next beams, the channel vector of i-th user in (3) can be rewritten as

$$\mathbf{h}_i = [h_{i,1}, ..., , h_{i,k}..., h_{i,N}] \triangleq \left(h_{i,k}^{\mathcal{D}} \quad \mathbf{h}_i^C \quad \mathbf{h}_i^F\right), \tag{9}$$

with $h_{i,k}$ denotes the k-th element of $\mathbf{h}_i$. Besides, in (9) we define that

- $h_{i,k}^{\mathcal{D}}$ represents the k-th feed, $k = 1, ..., N$, within the components of $\mathbf{h}_i$ that generates maximum gain toward i-th user, i.e., $h_{i,k}^{\mathcal{D}} = arg\ max\ \{\mathbf{h}_i\}$.
- The vector $\mathbf{h}_i^C \triangleq [h_{i,1}^C, ..., h_{i,c}^C, ..., h_{i,D_C}^C] \in \mathbb{C}^{1 \times D_C}$ where $h_{i,c}^C$ denotes the interference received by i-the user from c-th ($c = 1, ..., D_C$) user served at Close-Next beams.
- The vector $\mathbf{h}_i^F \triangleq [h_{i,1}^F, ..., h_{i,g}^F, ..., h_{i,D_F}^F] \in \mathbb{C}^{1 \times M}$ where $h_{i,g}^F$ denotes the interference received by i-the user from g-th ($g = 1, ..., D_F$) user located at Far-Next beams.

As stated above, the users located at Far-Next beams generate neglectable interference on i-th user. Therefore, to keep designing $\mathbf{W}$ computational complexity low, we can enforce $\mathbf{h}_i^F$ to be a zero vector, i.e.

$$h_{i,g}^F = 0 \qquad \forall g. \tag{10}$$

In the light words, the idea behind enforcing $\mathbf{h}_i^F$ to be zero in (10) comes from the fact that the Far-Next beams impose low or even neglecteable interference on i-th user due to their far footprint and side lobes of radiation pattern with the beams which serves i-th user. Note that the appropriate number of Close- and Far-Next beams with respect to each beam can be obtained through numerical results. In this context, given (10), the channel vector in (9) can be rewritten as

$$\mathbf{h}_{\mathcal{D},i} \triangleq \left(h_{i,k}^{\mathcal{D}} \quad \mathbf{h}_i^C \quad \mathbf{0}\right). \tag{11}$$

Indeed, $\mathbf{h}_{\mathcal{D},i}$ is the modified version of $\mathbf{h}_i$ in (9) employing (10). Then, for a set of M users the channel matrix in (3) can be then written as

$$\mathbf{H}_{\mathcal{D}} = [\mathbf{h}_{\mathcal{D},1}^H, ..., , \mathbf{h}_{\mathcal{D},i}^H, ..., \mathbf{h}_{\mathcal{D},M}^H]. \quad (12)$$

B. Reducing CSI Acquisition Complexity

In case of cosidering time varying channel matrix $\mathbf{H}$, the perturbation is appeared in channel matrix $\mathbf{H}_{\mathcal{D}}$ where the transmitting segment do not longer have access to the CSI of $\mathbf{H}_{\mathcal{D}}$ in (12) but to a degraded version such as [8]

$$\mathbf{H}_{\mathcal{D}} = \hat{\mathbf{H}}_{\mathcal{D}} + \mathbf{\Delta H}_{\mathcal{D}}, \quad (13)$$

where $\hat{\mathbf{H}}_{\mathcal{D}}$ represents the mean channel response with respect to the random user locations of $\mathbf{H}_{\mathcal{D}}$. Perturbation matrix $\mathbf{\Delta H}_{\mathcal{D}}$ models the difference between the actual and its mean values. We assume that the actual matrix $\mathbf{H}_{\mathcal{D}}$ relies on the neighborhood of the nominal channel matrices $\hat{\mathbf{H}}_{\mathcal{D}}$ that is known to the satellite. In particular, $\mathbf{H}_{\mathcal{D}}$ belongs to the uncertainty regions $\mathcal{H} = \{||\mathbf{H}_{\mathcal{D}} - \hat{\mathbf{H}}_{\mathcal{D}}|| \leq \omega_{\mathbf{\Delta H}_{\mathcal{D}}}\}$ which is a sphere centered at $\omega_{\mathbf{\Delta H}_{\mathcal{D}}}$. Interestingly, the channel model in (13) resembles the modeling of a MIMO system with imperfect CSI at the transmitter which has been solved as a worst case optimization problem in [9]-[10]. With this perspective, next subsection provides a worst case design of $\mathbf{W}$ in (8), which leads to a maxmin or minmax formulation. In this context, the Mean Square Error (MSE) for M users becomes

$$\mathbf{MSE} = \mathrm{E}\{|(\hat{\mathbf{s}} - \mathbf{s})|^2\},\ \hat{\mathbf{s}} \triangleq (\sqrt{\alpha})^{-1}\mathbf{y}, \quad (14)$$

C. Designing $\mathbf{W}$

Assuming (8), the performance metric Sum MSE (SMSE) for this MSE formulation is calculated by

$$\text{SMSE} = \text{trace}\left(\mathrm{E}\{(\hat{\mathbf{s}} - \mathbf{s})(\hat{\mathbf{s}} - \mathbf{s})^H\}\right) = \text{trace}\left\{\mathrm{E}(\mathbf{H}\mathbf{W}_b\mathbf{s}+\mathbf{n}-\mathbf{s})(\mathbf{H}\mathbf{W}_b\mathbf{s}+\mathbf{n}-\mathbf{s})^H\right\}. \quad (15)$$

Given (15), with employing the channel decomposition in (13), the minmax formulation of SMSE in (15) is obtained as

$$\begin{aligned} \min_{\mathbf{W}_b} \max_{\mathbf{\Delta H}_{\mathcal{D}}} \quad & \text{trace}\left\{\mathrm{E}\left((\mathbf{H}\mathbf{W}_b\mathbf{s}+\mathbf{n}-\mathbf{s})(\mathbf{H}\mathbf{W}_b\mathbf{s}+\mathbf{n}-\mathbf{s})^H\right)\right\} \\ s.t. \quad & ||\mathbf{H}_{\mathcal{D}} - \hat{\mathbf{H}}_{\mathcal{D}}|| \leq \omega_{\mathbf{\Delta H}_{\mathcal{D}}} \\ & \text{trace}(\mathbf{W}_b\mathbf{W}_b^H) \leq P. \end{aligned} \quad (16)$$

For a moment, let us consider that

$$\mathbf{H} = \mathbf{H}_{\mathcal{D}}. \quad (17)$$

With employing (17), the SMSE in (15) can be rewritten as

$$\text{SMSE} = \text{trace}\left[\left((\bar{\mathbf{H}}_{\mathcal{D}}\mathbf{W}_b - \mathbf{I}) + \mathbf{\Delta H}_{\mathcal{D}}\mathbf{W}_b\right)\left((\bar{\mathbf{H}}_{\mathcal{D}}\mathbf{W}_b - \mathbf{I}) + \mathbf{\Delta H}_{\mathcal{D}}\mathbf{W}_b\right)^H\right] + N. \quad (18)$$

With employing Lemma 7.1 in [9] and applying some mathematical manipulation, the SMSE in (18) is upper bounded by

$$\begin{aligned} \text{SMSE} \leq \widetilde{\text{SMSE}} \triangleq \text{trace}\left[(\bar{\mathbf{H}}_{\mathcal{D}}\mathbf{W}_b - \mathbf{I})(\bar{\mathbf{H}}_{\mathcal{D}}\mathbf{W}_b - \mathbf{I})^H + \epsilon_w\mathbf{W}_b\mathbf{W}_b^H\right], \\ + N = \mathbf{W}_b(\bar{\mathbf{H}}_{\mathcal{D}}\bar{\mathbf{H}}_{\mathcal{D}}^H + \epsilon_\omega\mathbf{I})\mathbf{W}_b^H + \mathbf{I} - \mathbf{W}_b\bar{\mathbf{H}}_{\mathcal{D}} - \bar{\mathbf{H}}_{\mathcal{D}}^H\mathbf{W}_b^H + N, \end{aligned} \quad (19)$$

where $\epsilon_w \triangleq \omega_{\mathbf{\Delta H}}^2 + \omega_{\mathbf{\Delta H}}\sigma_{max}(\bar{\mathbf{H}}_{\mathcal{D}}) + 2\omega_{\mathbf{\Delta H}}$. Indeed, the upper bound of SMSE in (19) is a direct consequence of the following bounds:

$$\mathbf{\Delta H}_{\mathcal{D}}^H\mathbf{\Delta H}_{\mathcal{D}}\mathbf{W}_b\mathbf{W}_b^H \leq \omega_{\mathbf{\Delta H}}^2\mathbf{W}_b\mathbf{W}_b^H, \quad (20)$$

$$\mathbf{\Delta H}_{\mathcal{D}}^H\bar{\mathbf{H}}_{\mathcal{D}}\mathbf{W}_b\mathbf{W}_b^H + \bar{\mathbf{H}}_{\mathcal{D}}^H\mathbf{\Delta H}_{\mathcal{D}}\mathbf{W}_b\mathbf{W}_b^H \leq 2\omega_{\mathbf{\Delta H}}\sigma_{max}(\bar{\mathbf{H}}_{\mathcal{D}})\mathbf{W}_b\mathbf{W}_b^H, \quad (21)$$

$$\mathbf{\Delta H}_{\mathcal{D}}\mathbf{W}_b + \mathbf{\Delta H}_{\mathcal{D}}^H\mathbf{W}_b^H \geq -2\omega_{\mathbf{\Delta H}}\sigma_{max}(\mathbf{A})\mathbf{W}_b\mathbf{W}_b^H, \quad (22)$$

where $\mathbf{A} \triangleq \mathbf{W}_b(\mathbf{W}_b^H\mathbf{W}_b)^{-1}$. We assume $\sigma_{\max}(\mathbf{A}) = 1$ in (24), and calculation optimal value for $\sigma_{\max}(\mathbf{A})$ is left for future.

Then, the matrix $\mathbf{W}_b$ which can be decreased the SMSE in (19) is designed as

$$\mathbf{W}_b = \sqrt{\alpha}\bar{\mathbf{H}}_{\mathcal{D}}^H(\bar{\mathbf{H}}_{\mathcal{D}}\bar{\mathbf{H}}_{\mathcal{D}}^H + \epsilon_\omega\mathbf{I})^{-1} \quad (23)$$

which reduces the $\widetilde{\text{SMSE}}$ in (19) to [1]

$$\widetilde{\text{SMSE}} = \text{trace}(\mathbf{I} + \bar{\mathbf{H}}_{\mathcal{D}}^H(\epsilon_\omega\mathbf{I})^{-1}\bar{\mathbf{H}}_{\mathcal{D}})^{-1}. \quad (24)$$

Indeed, the $\mathbf{W}_b$ in (23) is a traditional Zero Forcing (ZF) precoding scheme by adding a regularized factor $\epsilon_\omega\mathbf{I}$.

However, the design of $\mathbf{W}_b$ in (23) is done considering the naive assumption in (8) and this design will no longer valid while the objective of designing $\mathbf{W}$ is jointly constructing $\mathbf{W}_a$, $\mathbf{W}_b$ and $\mathbf{W}_c$. This joint design is the objective in the rest of this section.

In this context, we propose the following design of $\mathbf{W}_a$ and $\mathbf{W}_c$: *both $\mathbf{W}_c$ and $\mathbf{W}_a$ are zero matrices with single one at each row such that the position of one at each row of $\mathbf{W}_c$ and $\mathbf{W}_a$ respectively indicate the symbol transmitted to each user and the feed that serves corresponding user.*

Algorithm 1 presents a feed selection mechanism in order to determine appropriate place of one at i-th row of $\mathbf{W}_a$ to serve i-th user. Indeed, guarantees selecting the feed with maximum gain toward the i-th user ($i = 1, ..., M$). Furthermore, the position of the one at each row of $\mathbf{W}_c$ can be determined upon requested traffic through each user.

In such a design, $\mathbf{W}_b$ can be designed similar to (23) with the following modification:

$$\mathbf{W}_b = \mathbf{H}_{\mathcal{M}}^H(\mathbf{H}_{\mathcal{M}}\mathbf{H}_{\mathcal{M}}^H + \epsilon_\omega\mathbf{I})^{-1}, \quad (25)$$

$$\mathbf{H}_{\mathcal{M}} \triangleq \mathbf{W}_a\mathbf{H}_{\mathcal{D}}, \quad (26)$$

IV. Numerical Results

A. Simulation Setup

In order to compare the performance of the proposed techniques in Section III, Monte Carlo simulations are presented here. The simulation setup is based on an array fed reflector antenna/ feed provided by ESA with $K = N = 71$ feeds and beams which serve Europe territory [8]. Results have been averaged for a total of 500 channel realizations. The detail of simulation parameters are collected in Table I.

As a performance metric, we compute the SINR for each user, after interference mitigation and then its throughput (bit/s) is inferred according to DVB-S2x standard for a Packet Error Rate (PER) of 10^{-6} [12]. Note that this relationship has been obtained from [12] considering the PER curves. With this, the average total throughput at M users served by N feeds, one feed per user, becomes [8]

$$R_{\text{DVB-S2X}} = \frac{B_W}{1 + \eth}\sum_{i=1}^{M} f_{\text{DVB-S2X}}(\text{SINR}_i), \quad (27)$$

where $f_{\text{DVB-S2X}}(\cdot)$ is function that provides the DVB-S2x spectral efficiency for a given SINR. The scalar $\eth$ is the Roll-off factor. The term B_{W} denotes the total available bandwidth

[1] For arbitrary matrices $\mathbf{A}$, $\mathbf{B}$ and $\mathbf{C}$ we have [11]: $(\mathbf{A} + \mathbf{BC})^{-1} = \mathbf{A}^{-1} - \mathbf{A}^{-1}\mathbf{B}(\mathbf{I} + \mathbf{C}\mathbf{A}^{-1}\mathbf{B})^{-1}\mathbf{C}\mathbf{A}^{-1}$

Algorithm 1: Calculating matrix $\mathbf{W}_a$.

Data: Matrix $\mathbf{H}_{\mathcal{D}}$
Result: Matrix $\mathbf{W}_a$
Initialize;
Zero matrix $\mathbf{W}_a = [\mathbf{w}_{a,1}^H, ..., \mathbf{w}_{a,i}^H, ..., \mathbf{w}_{a,M}^H]^H$ where $\mathbf{w}_{a,i}$ is the i-th row of $\mathbf{W}_a$. The $\mathbf{w}_{a,i}$ is a zero vector.
Then;
for *i=1, ... ,M* **do**

a- Calculate

$$\mathbf{H}_{\mathcal{D}} = \left[\mathbf{h}_{\mathcal{D},1}^H, ..., \mathbf{h}_{\mathcal{D},i}^H, \ldots, \mathbf{h}_{\mathcal{D},M}^H\right].$$

where $\mathbf{h}_{\mathcal{D},i} \in \mathbb{C}^{1\times N}$ is the the channel vector of the i-th user;

b- Compute $\mathbf{h}_{\mathcal{D},i} = [h_{i,1}, \ldots, h_{i,k}, \ldots, h_{i,N}]$ where $h_{i,k}$ refers to the channel gain at i-th user from k-th, $k = 1, ..., N$, feed of the satellite;

c- In $\mathbf{h}_{\mathcal{D},i}$ find the the feed with maximum gain toward i-th user,i.e.

$$pos_i \triangleq arg\ max\ \{h_{i,1}, \ldots, h_{i,k}, \ldots, h_{i,N}\}$$

where pos_i denotes the feed number that generates maximum gain toward i-th user;

d- Fill the pos_i-th element of $\mathbf{w}_{a,i}$ with one as the selected feed to serve i-th user;

f- $i \leftarrow (i+1)$ Repeat;

End

TABLE I
SIMULATION PARAMETERS

Parameter	Value
Satellite position	$10^\circ East$
Frequency	20×10^9
Feed radiation pattern	Provided by ESA [8]
Number of feeds and beams	71
Carrier frequency	20 GHz (Ka band)
Total bandwidth	500 MHz
Atmospheric fading	Just rain fading [8]
Roll-off factor	0.25
User antenna gain	41.7 dBi

in the user link. For a best practice and in order to clarify the performance of proposed schemes, we consider two reference scenarios:

Reference 1: Conventional on-board ZF techniques to design $\mathbf{W}$ as

$$\mathbf{W} = \sqrt{\alpha}\mathbf{H}^H(\mathbf{H}\mathbf{H}^H)^{-1}. \quad (28)$$

Note that, to design $\mathbf{W}$ in (28), a real time CSI quantization mechanism is required between at the payload. In addition, similar to the assumption in (8), this design can not provide signal switching and feed selection possibilities.

Reference 2: A four frequency reuse pattern is considered. Indeed, with using this scheme the average throughput in (27) becomes $R_{\text{DVB-S2X,4C}} = \frac{B_W}{4(1+\delta)} \sum_{i=1}^{M} f_{\text{DVB-S2X}}(\text{SINR}_i)$.

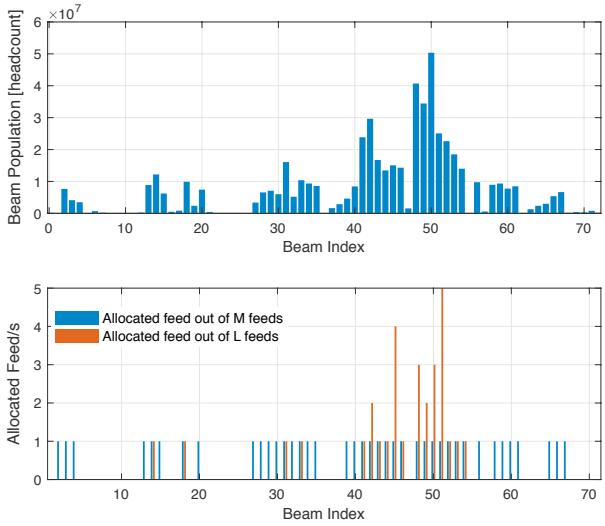

Fig. 2. [Up] Beam population for which the footprint is shown in Fig. 1. [Down] The feed distribution over each beam.

B. Complexity Analysis

Comparing the conventional design of $\mathbf{W}$ in (28) with the proposed one in (5) the following points are realized:

(i) Flexibility: the $\mathbf{W}$ in (28) suffers from the lake of signal switching and feed selection possibilities. In contrast, $\mathbf{W}$ in (5) contains aforementioned flexibilities.

(ii) Precoding computational complexity: while deploying precoding in (28) requires obtaining real time CSI of channel matrix $\mathbf{H}$ at the payload, the proposed scheme in (5) requires no CSI quantization mechanism at the payload. Indeed, the components which construct the precoding in (5) are robust to the channel variation. In addition, the channel matrix employed in (28) has KN non zero elements. In contrast, designing $\mathbf{W}_b$ requires only the information of $\mathbf{H}_{\mathcal{D}}$ which has $K(N-L)$ non zero elements by enforcing $\mathbf{h}_i^F$ in (11) to be zero, leading to lower operational complexity at (5) with respect to (28).

C. Results

To better show the benefits of applying proposed in (5), we consider the following definitions:

Offered Capacity per Beam (OCB): capacity/throughput that is delivered to each beam.

Demanded Capacity per Beam (DCB): the throughput/capacity requested by the users at each beam which can be defined for i-th beam as $\text{DCB}_i = QS_i$, with S_i refers to the population weight at i-th beam. Q is a tentative benchmark reference sealed capacity value to each beam which can be provided by satellite service providers. We consider $Q = 2.6$ [Gb/s].

UnMet Capacity per Beam: this capacity refers to the unserved demand at each beam and for i-th beam becomes $(DCB_i - OCB_i)^+$. *UnuSed Capacity per Beam:* the capacity of the satellite system that is not exploited at each beam and for i-th beam becomes $(OCB_i - DCB_i)^+$.

Figure 2 (Top) depicts the population distribution for the beams depicted in Fig. 1. It is seen that some beams have high

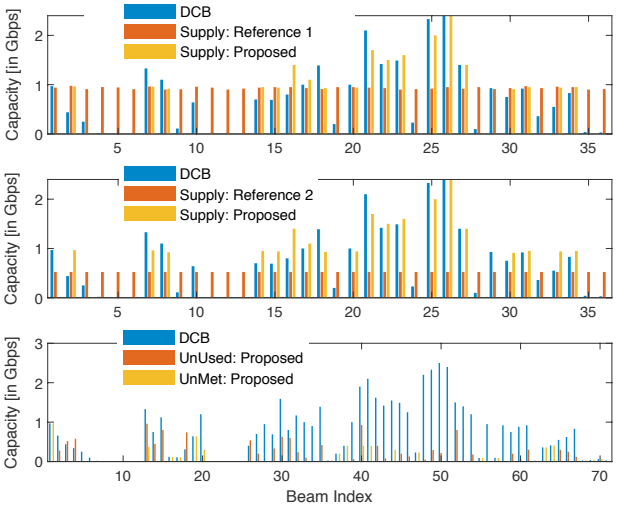

Fig. 3. Throughput (Gb/s) comparison among reference scenario 1 (Top) and 2 (Middle), as well as JPFS in (5). The distribution of UnMet and UnUsed capacities (Bottom).

TABLE II
PERFORMANCE COMPARISON BETWEEN JPFS AND REFERENCE SCENARIOS

Configurations	Average OCB	UnUsed	UnMet
Reference 1	89.39	14.33	4.11
Reference 2	71.56	11.46	8.09
Proposed	94.66	5.16	2.57

population, in contrast, some others have either no population or very low population. Therefore, we can avoid allocating on-board resources to the beams with low population and re-allocate these resources to the beams with high population, leading to have overlapping coverage of feeds at the beams with high population. Figure 2 (Bottom) shows the re-allocation of the feeds obtained from beams with low population. Clearly, the beams with high population serves through multiple feeds, with individual traffic stream per feed, such that L_1 users can obtain unicast service and L_2 users broadcast one which are distributed within the beams. Note that this re-allocation of the payload can be done through employed $\mathbf{W}_a$ and $\mathbf{W}_c$.

Figure 3 (Top and Middle) presents the throughput comparison among reference 1 and 2 as well as the proposed JPFS configuration in (5). As it is expected, the reference 1 and 2 provide a constant throughput over each beam without taking into account the effect of demand at each beam. Therefore, these two techniques present poor performance in the sense of UnMet and UnUsed capacities at each beam. In contrast, the proposed JPFS in (5) provides acceptable performance as well as it shows well functionality in order to decrease UnMet and UnUsed capacity at each beam.

Last but not least, the results in Fig. 3 (Top and Middle) is also justified by Fig. 3 (Bottom) and Table. II while employing JPFS in (5) provides lower UnMet and UnUsed capacities at each beam, with respect to other scenarios.

V. CONCLUSION

This paper designs less-complex on-board JPFS scheme in a multiple gateway multibeam satellite system employing full frequency reuse. The proposed design facilitates flexibility in resource allocation as well as a number of advantages over conventional payload. First, CSI exchange mechanism among the gateways and satellite is not required. Second, in case one gateway failure, rerouting signals through other gateways can be applied with no extra signal processing. Third, selecting on-board feed/s to serve each user which generates maximum gain toward corresponding user. Forth, flexibly switching the signals received from the gateways to requested users where each user can dynamically request traffic from any gateway. It is shown that since applying any on-board processing imposes computational complexity to the payload, the complexity of JPFS comes from: i) computational complexity of calculating the components included in JPFS itself, (ii) acquiring real time CSI at the satellite while channel matrix is time varying. In this context, JPFS deployed while an acceptable trade off between (i)-(ii) and performance was targeted.

ACKNOWLEDGMENT

This work was partially supported by the National Research Fund, Luxembourg under the projects "FNR-DPSAT" and "FNR-PROSAT".

REFERENCES

[1] G. Verelst *et al.*, *"Innovative System Architecture to reach the Terabit/s Satellite,"* in 31st AIAA International Communications Satellite Systems Conference (ICSSC), Florence, IT, Oct. 2013.
[2] Daniel Minoli, *"Innovations in satellite communications technology,"* in John Wiley&Sons Inc. Hoboken, USA, 2015.
[3] M. A. Vazquezi *et al.*, *"Precoding in Multibeam Satellite Communications: Present and Future Challenges,"* in IEEE Wireless Commun., vol. 23, no. 6, pp. 88-95, Dec. 2016.
[4] D. Christopoulos, S. Chatzinotas, and B. Ottersten, *"Full frequency reuse multibeam satellite systems: Frame based precoding and user scheduling,"* in IEEE Trans. Wireless Commun., 2015 (submitted).
[5] V. Joroughi, M. A. Vzquez and A. I. Prez-Neira, *"Precoding in multigateway multibeam satellite systems,"* in IEEE Trans. Wireless Commun., vol. 15, no. 7, pp. 1-13, Jul. 2016.
[6] G. Zheng, S. Chatzinotas and B. Ottersten, *"Multi-gateway cooperation in multibeam satellite systems,"* in 23rd IEEE PIMRC, 2012, USA.
[7] V. Joroughi *et al.*, *"Design of an on board beam generation process for a multibeam broadband satellite system,* in IEEE Trans. Wireless Commun., vol. 13, pp. 1-14, Mar. 2017.
[8] ESA, 23089/10/NL/CPL, *"Satellite Network of Experts (SatNEx) IV,"* https://satnex4.org.
[9] D. Palomar, J. Cioffi and M. A. Lagunas, *"Joint Tx-Rx beamforming design for multicarrier MIMO channels: a unified framework for convex optimization,"* in IEEE Trans. Sig. Process., vol. 51, no. 9, pp. 2381-2401, Sep. 2003.
[10] D. P. Palomar *"A unified framework for communications through MIMO channels,"* in Ph.D. dissertation, Technical University of Catalonia (UPC), May 2003, Spain.
[11] G. H. Golub and C. F. Van Loan, *"Matrix computations (3rd Ed.)*in Johns Hopkins University Press, 1996, USA.
[12] ETSI TR 102 37, *"DVB-S2x: Digital video broadcasting user guidelines for second generation system for broadcasting interactive services, news gathering and other broadband satellite application,"*.